Mach stem formation in reflection and focusing of weak shock acoustic pulses

Maria M. Karzova[a)] and Vera A. Khokhlova[b)]
*Department of Acoustics, Faculty of Physics, Moscow State University, Leninskie Gory,
Moscow 119991, Russia
masha@acs366.phys.msu.ru, vera@acs366.phys.msu.ru*

Edouard Salze, Sébastien Ollivier, and Philippe Blanc-Benon
*Laboratoire de Mécanique des Fluides et d'Acoustique, Unité Mixte de Recherche 5509,
Centre National de la Recherche Scientifique, Ecole Centrale de Lyon, Université Lyon I,
36 Avenue Guy de Collongue, F-69134 Ecully Cedex, France
edouard.salze@ec-lyon.fr, sebastien.ollivier@univ-lyon1.fr, philippe.blanc-benon@ec-lyon.fr*

Abstract: The aim of this study is to show the evidence of Mach stem formation for very weak shock waves with acoustic Mach numbers on the order of 10^{-3} to 10^{-2}. Two representative cases are considered: reflection of shock pulses from a rigid surface and focusing of nonlinear acoustic beams. Reflection experiments are performed in air using spark-generated shock pulses. Shock fronts are visualized using a schlieren system. Both regular and irregular types of reflection are observed. Numerical simulations are performed to demonstrate the Mach stem formation in the focal region of periodic and pulsed nonlinear beams in water.
© 2015 Acoustical Society of America
[DKW]

1. Introduction

Ernst Mach was the first scientist who experimentally observed the phenomenon of shock wave reflection.[1] In his experiments, reported in 1878, he recorded two different shock wave reflection patterns. The first one is regular reflection, which shows the incident and reflected shocks intersecting right at the reflecting surface. The second type of reflection, known as irregular reflection, consists of three shocks [Fig. 1(a)]: the incident and the reflected shocks which intersect above the surface, and a third one, later named the Mach stem, which connects the intersection point with the surface.[2]

Theoretical investigation of the shock wave reflection was first carried out by von Neumann in 1943.[3] He described the irregular reflection by a three-shock theory based on the assumption that all the waves in the flow are shaped as shocks of negligible curvature and thickness, and obey the Rankine-Hugoniot jump conditions. The three-shock theory was found to be in good agreement with experiments only for strong shocks when the acoustic Mach number M_a (defined as the ratio of the maximum particle velocity in acoustic wave to the ambient sound speed in the propagation medium) was greater than 0.47.[4] For weak shocks ($M_a < 0.05$) the three-shock theory has no physically acceptable solutions, while experimental observations supported by numerical simulations clearly show that irregular type of reflection for such weak shocks does, in

a)Also at: Laboratoire de Mécanique des Fluides et d'Acoustique, Unité Mixte de Recherche 5509, Centre National de la Recherche Scientifique, Ecole Centrale de Lyon, Université Lyon I, 36 Avenue Guy de Collongue, F-69134 Ecully Cedex, France.

b)Also at: Center for Industrial and Medical Ultrasound, Applied Physics Laboratory, University of Washington, 1013 NE 40th Street, Seattle, WA 98105, USA.
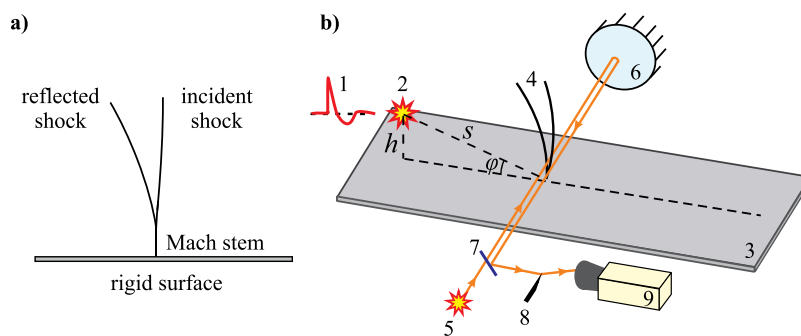
Fig. 1. (Color online) (a) Sketch illustrating the irregular type of reflection. (b) Illustration of the experimental setup: 1—shock acoustic pulse, 2—a spark source, 3—a rigid surface, 4—reflection pattern consisting of incident and reflected fronts, 5—QTH continuous light source, 6—a spherical mirror, 7—a beam splitter, 8—an optical knife, and 9—a high-speed camera (Phantom V12 CMOS). Solid lines with arrows illustrate the trajectory of the light beam in the absence of acoustic wave.

fact, exist.[4] The conflict between three-shock theory and experimental results is known as the von Neumann paradox, and irregular reflection pattern in this case is called the von Neumann reflection. Existing studies to resolve the von Neumann paradox are mainly in the framework of aerodynamics and consider only step shocks with acoustic Mach numbers M_a greater than 0.035.[5–9] While step shocks are typical for aerodynamics, acoustic shock waves usually have more complicated waveforms of an N-wave (sonic boom waves), blast waves, sawtooth waves, and others. In addition, in nonlinear acoustics the values of acoustic Mach number M_a are on the order of 10^{-3}, which is at least one order smaller than in aerodynamics. The reflection of such very weak, but nonetheless strongly nonlinear acoustic waves has not been studied to the same extent.

Nonlinear reflection of acoustic shock waves from a rigid surface was investigated numerically in a recent work (Ref. 10), where cases of an ideal plane N-wave and periodic sawtooth wave were studied in comparison with a step shock. It was shown that depending on the value of a critical parameter a introduced as $a = \sin\varphi/\sqrt{2\beta M_a}$ (here φ is the grazing angle of the incident wave and β is the coefficient of nonlinearity of the propagation medium) the type of reflection could vary from weak von Neumann reflection to von Neumann reflection and finally to a regular reflection.[10] The term "weak von Neumann reflection" was introduced by the authors of Ref. 10 to describe the reflection pattern for almost grazing incidence when the reflected shock does not exist, but the initial plane incident shock has a curvature close to the surface. The von Neumann reflection is an irregular reflection regime characterized mainly by the continuous slope of the shock front along the incident shock and the Mach stem.[4] These types of reflection were successfully observed experimentally for periodic sawtooth waves ($M_a = 2.3 \times 10^{-4}$) in water,[11] and values of the critical parameter a corresponding to each reflection regime were determined. Irregular reflection of spherically divergent spark pulses was observed in numerical experiments,[12] but no quantitative analysis of values of the critical parameter a was done.

Mach stem formation for acoustic weak shock waves occurs not only in the case of reflection from rigid boundaries, but it can also be observed in other interactions of two shock fronts. Focusing of axially symmetric beams is the situation most similar to the reflection from the rigid surface: the normal derivative of the pressure on the axis of focused beam and at the rigid surface in reflection wave pattern is equal to zero. Thus, one can expect a process similar to Mach stem formation in the focal region of nonlinear beams. For step shock cases the Mach stem formation was indeed observed experimentally[13] and in simulations[9] for focusing of shocks. The process of two shock collision in one period of a continuous wave generated by a plane piston source was studied numerically,[14] but it was not considered as similar to Mach stem

formation process and thus the structure of the wavefronts in the region of weak shock interaction was not shown.

In this letter, we focus on interactions of shock fronts when waves are (i) very weak (M_a is on the order of 10^{-3} to 10^{-2}), (ii) have waveforms typical for acoustics (*N*-waves, sawtooth waves, and bipolar pulses). The goals are to demonstrate experimentally how irregular reflection occurs in air for very weak spherically diverging spark-generated pulses resembling the *N*-wave and to evaluate the values of the critical parameter *a* for different types of reflection. This complements earlier experimental observations on irregular reflections of plane periodic waves in water (Ref. 11) since spherical divergent waves, single pulses, propagation in air, and variation in acoustic Mach number were considered. The qualitative analogy of the Mach stem formation in a focal region of nonlinear periodic and pulsed ultrasound beams was demonstrated numerically in water using the Khokhlov-Zabolotskaya-Kuznetsov (KZK) equation.

2. Nonlinear reflection of spark-generated shock pulses in air: Optical measurements

The experimental setup designed for optical visualization of shock wave reflection from a rigid surface is shown in Fig. 1(b). Acoustic shock waves (1) were produced by a 15 kV electric spark source (2) with 21 mm gap between tungsten electrodes (its calibration is described in detail in a previous paper).[15] The generated wave (1) was a short pulse of about 30 μs duration, beginning with a shock front followed by a narrow compression phase and then by a smooth rarefaction phase. Spherically divergent acoustic pulses reflect from the rigid surface (3), located at a distance *h* under the spark. The emerging reflection pattern (4) was visualized using a schlieren method.[16] The schlieren system was composed of a quartz tungsten halogen (QTH) continuous white light source (5) mounted in the geometrical focus of a spherical mirror (6) with 1 m radius of curvature, a beam splitter (7), an optical knife (a razor edge, 8), and a high-speed Phantom V12 CMOS camera (9) with exposure time set to 1 μs. Light beam was transmitted through the beam splitter (7) and through the test zone of the acoustic pulse reflection. Then, the light reflected from the mirror (6), intersected the test zone once again, and propagated back to the beam splitter [solid lines with arrows in Fig. 1(b)]. Spatial variations of the light refractive index *n* caused by the acoustic wave led to deviation of part of light rays from the initial propagation direction. Light rays that were not deflected by acoustic pressure inhomogeneities were blocked by the optical knife (8) located at the focus of the beam. Deflected rays bent around the razor edge (8) were captured by the high-speed camera (9) to form a schlieren image. Double passing of the light beam through the test zone provided better contrast of the image. Since the brightness of these images is proportional to the gradient of the acoustic pressure,[16] they depict qualitatively the reflection pattern of the front shock of the pulse.

For visualizing the reflection pattern, an initial series of schlieren images was recorded without acoustic wave to obtain the averaged background image. A second series of images was recorded with the presence of acoustic wave. Raw images in the second series were dark and the front structure was not clearly seen without additional data processing. The averaged background image was subtracted from every recorded image of the reflection pattern; this subtraction resulted in reduction of noise and enhancement of the image contrast. An additional processing was the averaging of twenty images obtained from different sparks for a fixed source and reflection point configuration. In these images, the position of the reflection point varied by less than 5 mm and the reflection patterns were juxtaposed before averaging. Schlieren images [(19.5 ± 0.2) mm width × (12.2 ± 0.2) mm height] of the reflection patterns obtained in this way are presented in Fig. 2.

In order to investigate independently the effect of the pressure level and the incident angle φ on the reflection pattern, we chose the position of the spark source so that the distance *s* between the source and the reflection point was the same for each angle φ considered in the study [Fig. 1(b)]. The results are given in Fig. 2 for two values of acoustic Mach number M_a (i.e., two distances *s* between the source and the
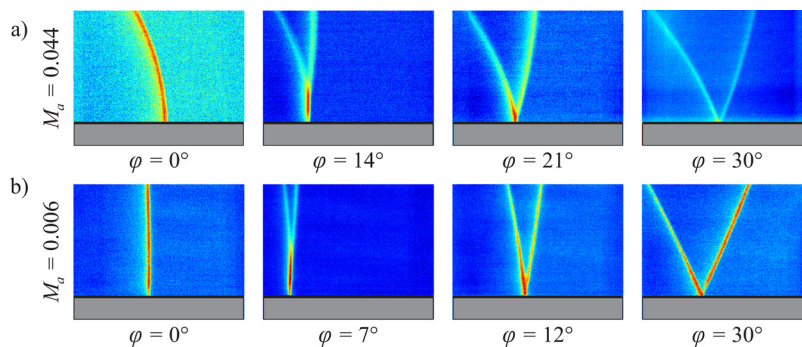
Fig. 2. (Color online) Optical visualization of a front shock reflection from a rigid surface. Reflection point is positioned 4.6 cm (a) and 20.7 cm (b) away from the spark source. The rigid surface is located in the bottom of each image; the wave propagates from left to right.

reflection point) and different values of the incident angle φ. The series of frames in Fig. 2(a) was obtained at a distance $s = (46 \pm 4)$ mm away from the spark source, which corresponded to an acoustic pressure amplitude for the incident wave $p_0 = (6.2 \pm 0.5)$ kPa and a value of the acoustic Mach number $M_a = (0.044 \pm 0.004)$. To estimate the value of the acoustic Mach number we used its definition for the plane wave: $M_a = p_0/\gamma p_{atm}$, where $\gamma = 1.4$ is the adiabatic index for air and $p_{atm} = 100$ kPa is the atmospheric pressure. For the series of frames in Fig. 2(b), experimental parameters were $s = (207 \pm 7)$ mm, $p_0 = (0.84 \pm 0.04)$ kPa, and $M_a = (0.0060 \pm 0.0003)$. The coefficient of nonlinearity β was equal to 1.2 for the experimental conditions of the relative humidity of 49% and temperature of 292 K.

For the grazing angle $\varphi = 0°$ the spark source was located right at the reflecting surface ($h = 0$). In this case no reflected shock was observed for both values of acoustic Mach number M_a (cases $\varphi = 0°$ in Fig. 2). The same pattern was achieved also for the angles $\varphi \leq 7°$ when $M_a = 0.044$ and for $\varphi \leq 5°$ when $M_a = 0.006$ (not shown here). Whether the absence of visible reflected shock is a confirmation of the weak von Neumann reflection regime or is the result of not enough sensitivity of the schlieren system still remains an open question. With further increasing the incident angle φ, one can clearly observe the irregular type of reflection with Mach stem formed close to the surface ($\varphi = 14°$ for $M_a = 0.044$ and $\varphi = 7°$ for $M_a = 0.006$). There were no visible slopes discontinuities between Mach stem and the incident shock which is a feature characteristic for von Neumann reflection. Then for $\varphi \geq 20°$ ($M_a = 0.044$) and $\varphi \geq 8°$ ($M_a = 0.006$) the regime of reflection is modified into regular reflection with incident and reflected shocks merged right at the surface [cases $\varphi = 21°$ and $30°$ in Fig. 2(a); $\varphi = 12°$ and $30°$ in Fig. 2(b)]. Experimental values of the critical parameter $a = \sin\varphi / \sqrt{2\beta M_a}$ corresponding to each observed reflection regime are given in Table 1. Note that within experimental error

Table 1. Experimental values of the critical parameter a for different types of reflection. Data were obtained for two distances from the spark source.

Experimental parameters		Weak von Neumann reflection	von Neumann reflection	Regular reflection
$M_a \times 10^{-2}$	4.4 ± 0.4	Probably occurs for $a \leq (0.38 \pm 0.05)$	$(0.38 \pm 0.05) < a < (1.05 \pm 0.15)$	$a \geq (1.05 \pm 0.15)$
s (mm)	46 ± 4			
p_0 (kPa)	6.2 ± 0.5			
$M_a \times 10^{-3}$	6.0 ± 0.3	Probably occurs for $a \leq (0.58 \pm 0.2)$	$(0.58 \pm 0.2) < a < (1.1 \pm 0.3)$	$a \geq (1.1 \pm 0.3)$
s (mm)	207 ± 7			
p_0 (kPa)	0.84 ± 0.04			

the transition between the different reflection regimes occurs for similar values of the critical parameter a.

Both amplitude p and grazing angle φ of the acoustic pulse change while the pulse propagates along the surface that leads to the change of the "current" value of the critical parameter a. As a result, the reflection pattern has a dynamic character changing with the propagation distance. This was confirmed in the experiment: the length of the Mach stem increased when the pulse propagated along the surface. For three consecutive schlieren images obtained at different distances from the spark along the surface (Fig. 3), both parameters M_a and φ were decreasing and therefore had different effect on the value of a. Increasing of the Mach stem length means that the value of a was decreasing and the variation of the grazing angle φ had stronger effect on a than the variation of the Mach number M_a.

3. Mach stem formation in focused nonlinear acoustic beams: Numerical modeling in water

Mach stem formation in the focal area of nonlinear periodic and pulsed ultrasound beams was demonstrated numerically using the KZK nonlinear evolution equation.[17] The equation is valid for small focusing angles and $M_a \ll 1$ which are exactly the cases of interest here. For axially symmetric beams the KZK equation can be written in dimensionless form as

$$\frac{\partial}{\partial \Theta}\left[\frac{\partial P}{\partial \sigma} - NP\frac{\partial P}{\partial \Theta} - A\frac{\partial^2 P}{\partial \Theta^2}\right] = \frac{1}{4G}\left(\frac{\partial^2 P}{\partial R^2} + \frac{1}{R}\frac{\partial P}{\partial R}\right). \tag{1}$$

Here $P = p/p_0$ is the acoustic pressure normalized by its initial amplitude p_0, $\sigma = x/F$ is the coordinate along the beam axis normalized by the focal length of the source F, $R = r/a_0$ is the radial propagation coordinate normalized by the radius of the source a_0, $\Theta = 2\pi\tau/T_0$ is the dimensionless time, $\tau = t - x/c_0$ is the retarded time, c_0 is the ambient sound speed, and T_0 is the duration of the signal (for a harmonic wave it is one period of wave). Equation (1) accounts for the combined effects of nonlinearity, diffraction, and absorption characterized, respectively, by three dimensionless parameters N, G, and A: $N = 2\pi F \beta p_0/\rho_0 c_0^3 T_0$ is the nonlinear parameter, where ρ_0 is the ambient density; $G = \pi a_0^2/c_0 F T_0$ is the diffraction parameter; and $A = 2\pi^2 bF/\rho_0 c_0^3 T_0^2$ is the absorption parameter, where b is the dissipation coefficient.[18] Equation (1) was solved numerically in finite differences using a previously developed algorithm.[14,19] The boundary condition was set as a piston focused source. Initial waveforms were a periodic harmonic wave and a bipolar pulse [Figs. 4(c) and 4(f), frames "initial"]. The dimensionless parameters in the modeling were $N = 1$, $G = 10$, and $A = 0.0054$, which are typical values for lithotripters and medical transducers used for therapy of soft tissues.[20]

First, consider results of modeling obtained for nonlinear propagation of focused periodic acoustic waves [Figs. 4(a)–4(c)]. It is clearly seen that the spatial structure of the wave front is very similar to the von Neumann reflection: it contains one front intersecting the beam axis (the Mach stem) further dividing into two fronts at each distance from the axis [Figs. 4(a) and 4(b)]. A continuous slope can be seen between the focusing front and the Mach stem that distinguishes the von Neumann reflection regime. Note that the Mach stem structure corresponds to one shock in one period of the wave [Fig. 4(c), waveform 1], while there are two shocks in one period of
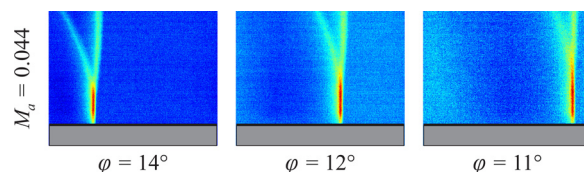

Fig. 3. (Color online) Three consecutive schlieren images from the high-speed camera obtained for the same position of the spark source ($M_a = 0.044$ for the first frame).
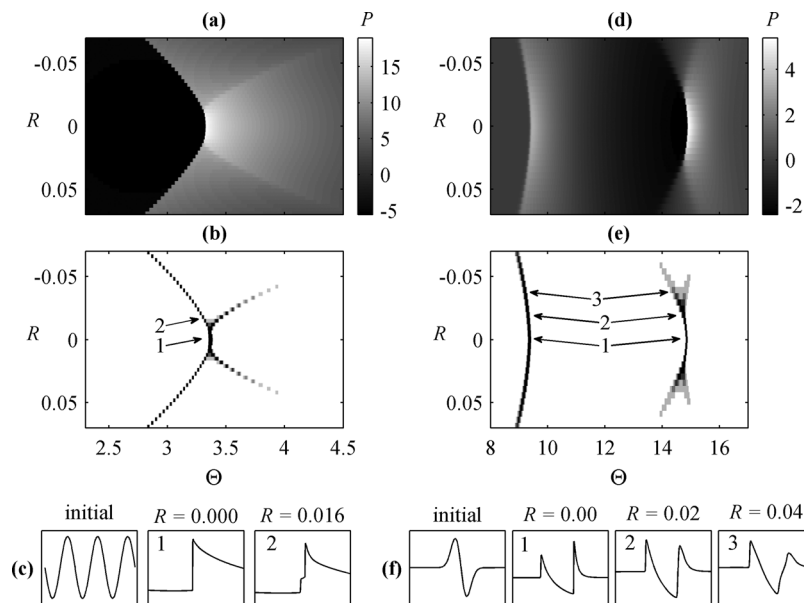
Fig. 4. Mach stem formation in the focused beams of periodic waves [(a)–(c)] and bipolar pulses [(d)–(f)]. (a), (d) Temporal pressure waveforms at different transverse distances R from the beam axis. (b), (e) Temporal derivatives of the pressure waveforms shown on (a) and (d) correspondingly, i.e., numerical schlieren images. The darker greys indicate higher values of the derivatives. (c), (f) Initial waveform and waveforms at different radial distances R from the axis indicated by arrows in (b) and (e) correspondingly.

the wave away from the axis at $R = 0.016$ [Fig. 4(c), waveform 2]. In Ref. 14 it was shown that for the two shock structure in one period of the harmonic wave, the higher shock is coming from the edge of the source, and the lower shock is coming from its central part. The formation of the Mach stem structure in the focal area of acoustic beams is thus the result of nonlinear interaction of shock fronts of the edge and central waves. These two fronts merge, because the velocity of the shock depends on its pressure,[6] the higher shock in the waveform propagates faster than the lower shock. These two shocks collide and the Mach stem forms in the beam region close to the axis.

In pulsed beams, the edge wave starts to collide with the central wave at the end of the pulse, therefore the second shock front and Mach stem structure form within an initially negative phase of the bipolar pulse [$14 < \Theta < 16$ in Figs. 4(d) and 4(e)]. The front pattern in this case also resembles the von Neumann reflection with continuous slope between the fronts of the central wave and the Mach stem [Fig. 4(d)], but the front structure is blurred [Fig. 4(e)]. Smearing of the front structure occurs since the edge wave in the pulsed fields is smoother than in the periodic fields [Fig. 4(f), rear shocks of waveform 2 and waveform 3] and thus the values of the pressure derivative are less. When the edge wave front merges with that of the central wave, they turn into a sharp shock and provide the excess of the pressure amplitude on the rear shock [Fig. 4(f), waveform 1]. This excess of the pressure is clearly observed as the white area in [Fig. 4(d)] at the location of the Mach stem structure.

4. Conclusion

In acoustics, interaction of shocks can occur in similar ways in reflection from a rigid surface and in focusing of axially symmetric nonlinear beams. In this paper, these two cases were considered for very weak (M_a within the range from 10^{-3} to 10^{-2}) acoustic waves of differing temporal structure (N-wave, sawtooth wave, and bipolar pulse). Reflection of N-waves was studied experimentally in air using an electric spark to create the acoustic wave and the schlieren system to visualize reflection patterns. Regular

and irregular types of reflection were observed, and corresponding values of the critical parameter *a* for each reflection regime were determined. Numerical simulations based on the KZK equation for nonlinear periodic and pulsed acoustic beams in water showed a process analogous to the Mach stem formation. The structure of the front patterns in the focal region of the beam resembled to the von Neumann reflection as the result of interaction between the edge and the central waves coming from the source. For pulsed beams the effect occurred only for the rear shock of the pulse.

Acknowledgments

References and links

[1] E. Mach, "Über den Verlauf von Funkenwellen in der Ebene und im Raume" ("Over the course of radio waves in the plane and in space"), Sitzungsbr. Akad. Wiss. Wien **78**, 819–838 (1878).

[2] G. Ben-Dor, *Shock Wave Reflection Phenomena* (Springer Verlag, New York, 1992), pp. 3–13.

[3] J. Von Neumann, "Oblique reflection of shocks," in *John von Neumann Collected Work*, edited by A. H. Taub (MacMillan, New York, 1963), Vol. 6, pp. 238–299.

[4] P. Colella and L. F. Henderson, "The von Neumann paradox for the diffraction of weak shock waves," J. Fluid Mech. **213**, 71–94 (1990).

[5] B. Skews and J. Ashworth, "The physical nature of weak shock wave reflection," J. Fluid Mech. **542**, 105–114 (2005).

[6] M. Brio and J. K. Hunter, "Mach reflection for the two-dimensional Burgers equation," Physica D **60**, 194–207 (1992).

[7] E. I. Vasiliev and A. N. Kraiko, "Numerical simulation of weak shock diffraction over a wedge under the von Neumann paradox conditions," Comput. Math. Phys. **39**, 1335–1345 (1999) [Zh. Vychisl. Mat. Mat. Fiz. **39**(8), 1393–1404 (1999)].

[8] A. R. Zakharian, M. Brio, J. K. Hunter, and G. M. Webb, "The von Neumann paradox in weak shock reflection," J. Fluid Mech. **422**, 193–205 (2000).

[9] E. G. Tabak and R. R. Rosales, "Focusing of weak shocks waves and the von Neumann paradox of oblique shock reflection," Phys. Fluids **6**, 1874–1892 (1994).

[10] S. Baskar, F. Coulouvrat, and R. Marchiano, "Nonlinear reflection of grazing acoustic shock waves: Unsteady transition from von Neumann to Mach to Snell-Descartes reflections," J. Fluid Mech. **575**, 27–55 (2007).

[11] R. Marchiano, S. Baskar, F. Coulouvrat, and J.-L. Thomas, "Experimental evidence of deviation from mirror reflection for acoustical shock waves," Phys. Rev. E **76**, 056602 (2007).

[12] V. W. Sparrow and R. Raspet, "A numerical method for general finite amplitude wave propagation in two dimensions and its application to spark pulses," J. Acoust. Soc. Am. **90**(5), 2683–2691 (1991).

[13] B. Sturtevant and V. A. Kulkarny, "The focusing of weak shock waves," J. Fluid. Mech. **73**, 651–671 (1976).

[14] V. A. Khokhlova, R. Souchon, J. Tavakkoli, O. A. Sapozhnikov, and D. Cathignol, "Numerical modeling of finite amplitude sound beams: Shock formation in the near field of a cw plane piston source," J. Acoust. Soc. Am. **110**(1), 95–108 (2001).

[15] P. Yuldashev, S. Ollivier, M. Averiyanov, O. Sapozhnikov, V. Khokhlova, and P. Blanc-Benon, "Nonlinear propagation of spark-generated N-waves in air: Modeling and measurements using acoustical and optical methods," J. Acoust. Soc. Am. **128**(6), 3321–3333 (2010).

[16] G. S. Settles, *Schlieren and Shadowgraph Techniques: Visualizing Phenomena in Transparent Media* (Springer-Verlag, Heidelberg, 2001), pp. 27, 39–52, 338–340.

[17] E. A. Zabolotskaya and R. V. Khokhlov, "Quasi-plane waves in the nonlinear acoustics of confined beams," Sov. Phys. Acoust. **15**, 35–40 (1969).

[18] O. V. Bessonova, V. A. Khokhlova, M. R. Bailey, M. S. Canney, and L. A. Crum, "Focusing of high power ultrasound beams and limiting values of shock wave parameters," Acoust. Phys. **55**, 463–476 (2009).

[19] M. M. Karzova, M. V. Averianov, O. A. Sapozhnikov, and V. A. Khokhlova, "Mechanisms for saturation of nonlinear pulsed and periodic signals in focused acoustic beams," Acoust. Phys. **58**(1), 81–89 (2012).

[20] M. R. Bailey, V. A. Khokhlova, O. A. Sapozhnikov, S. G. Kargl, and L. A. Crum, "Physical mechanisms of the therapeutic effect of ultrasound," Acoust. Phys. **49**(4), 369–388 (2003).